# LAYERS IN THE SLAG FILM BETWEEN STEEL SHELL AND MOULD IN CONTINUOUS CASTING OF STAINLESS STEEL

**Paavo Hooli**
Outokumpu Stainless Oy, Finland

## ABSTRACT

*In order to investigate the structure and properties of different slag layers in the mould gap sampling was carried out in the tail-out phase at the end of the cast. Several massive slag film samples were collected. The most typical feature in the sampled films was the layer dominated by a cuspidine phase. In the film cuspidine rich layer was locating next to the lubricating layer, and towards the mould surface this followed by a nepheline rich layer, then a NaF layer and finally a layer containing essentially elemental sodium next to the mould surface.*

*Analysis showed that the flux film structure could explain some industrial cases in which very low local heat transfer was observed. Properties of the slag film had also influence on the sticking frequency via fracturing in the film. The influence of the composition of casting powder and Ti alloying in steel on the formation of layers in the film are also discussed.*

*There was a tendency for those compounds of minor elements (impurities in powder, from steel or refractories, or added as tracer) to be distributed unevenly in the main phases. The main phases were for example cuspidine or nepheline, and minor elements were in this case Mg, Mn, Zr, S, K and Ti. Minor elements ("impurities") in the powder have tendency to favour certain phases and can also have influence on the formation of different phases.*

## INTRODUCTION

Overall heat transfer in the mould measured by temperature increase in cooling water is typically decreasing after the start of the casting. Sometimes this decrease can be prolonged to several hours when casting stainless steel. This decrease is not anyhow evenly distributed along the length of the mould.

A reason for the lowering heat transfer is the formation of solid slag film in the gap between the steel shell and the mould. This paper describes the structures found in the film, calculations of their influence on local heat transfer and comparison with measured values.

## SAMPLING AND CASTING POWDERS

Sampling was carried out in a tail-out phase at the end of cast. Several massive samples were collected. As shown in Figure 1, the best samples traversed almost the whole width of the wide faces. The slag rim can be seen at the top. Some of the samples reached down to 40 cm from the meniscus.

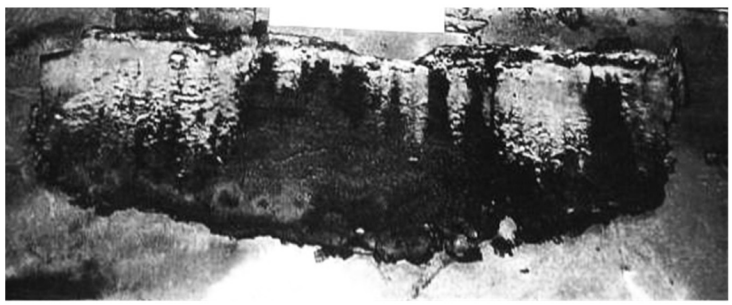

Figure 1: Photograph shows a sample. The sampled pieces were lifted on a low tray after sampling to maintain their correct placement following possible fracturing due to cooling. (Some fracturing always took place.)[2]. The width of this sample was about 1 m

Compositions of the used casting powders based on information provided by suppliers were as follows (ranges of main compounds): 30-32 mass% $SiO_2$, 32-37 mass% CaO, 5.3-6.8 mass% $Al_2O_3$, 7-9.3 mass% $Na_2O$, 0.4-0.7mass% $K_2O$ and 6.3-7.5 mass% F.

The steel grades were austenitic stainless AISI 300 series.

## FORMATION OF FILM

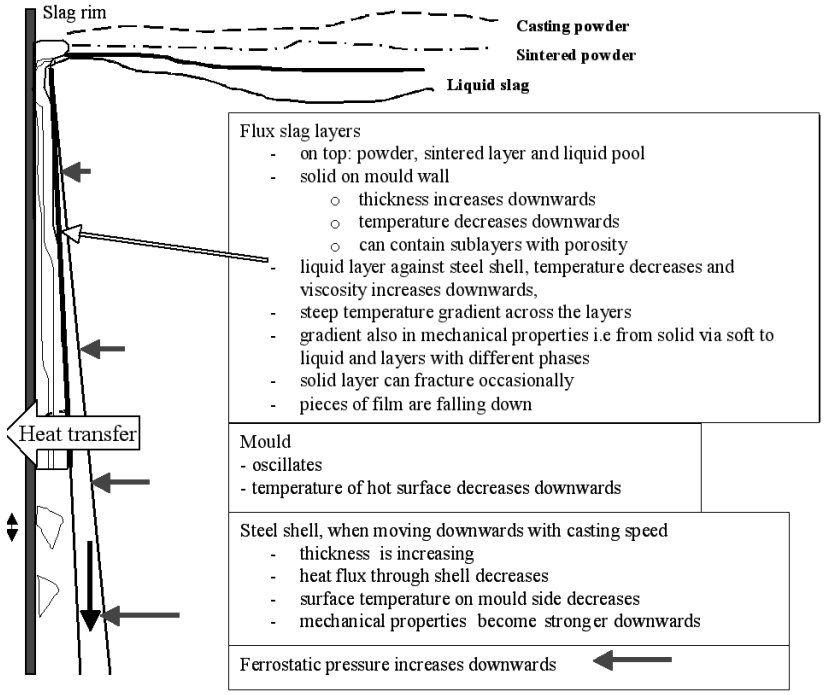


Figure 2: Schematic presentation of the conditions in the gap between mould and steel shell [1]

Conditions in the mould where the flux film is forming are complicated as presented in Figure 2.

The first solid layers on the mould wall are solidifying rapidly and the last solid layers on the shell side next to the liquid layer are solidifying very slowly. The first solid layers are probably solidifying as glassy but via a devitrification process they have a crystalline structure in most of the samples. Some films are shown in Figures 4B, 4C, 7, 8 and 10.

## MOULD SIDE SURFACE OF THE FILM

Characteristic features of the mould side surfaces of the sampled films included (see Figure 3):

- Uneven surfaces and colour variation
- Variation of concentrations of different elements
- Fractures and bleedings
- Glassy bleedings
- Wave lines resembling oscillation marks
- *Craters*
- Areas resembling netted patterns
- Areas with no Ca.

On the surface of a film shown in Figure 3 there are extra wide variety of colours. Different colours indicate different compositions; some areas contain shapes similar to oscillation marks, and others resemble volcanic craters. There were few areas showing bleeding.

The area marked with x in Figure 3 was examined with a magnification of 500, and different points (phases) were analysed with SEM/EDS. This revealed that the matrix phase was NaF together with a cuspidine phase, which had a needle-like form (lengths about 20-30 μm) and a multi-component compound containing O, Na, Cr, F, Si and Ca (in the order of concentrations). Separation of the phases had thus taken place on a small scale. In this area, *overall* concentrations of fluorine and sodium were high (26% F and 26% Na) (composition 2: 16% O, 26% F, 26% Na, 6% Si, 9% Ca, 6% Mn).

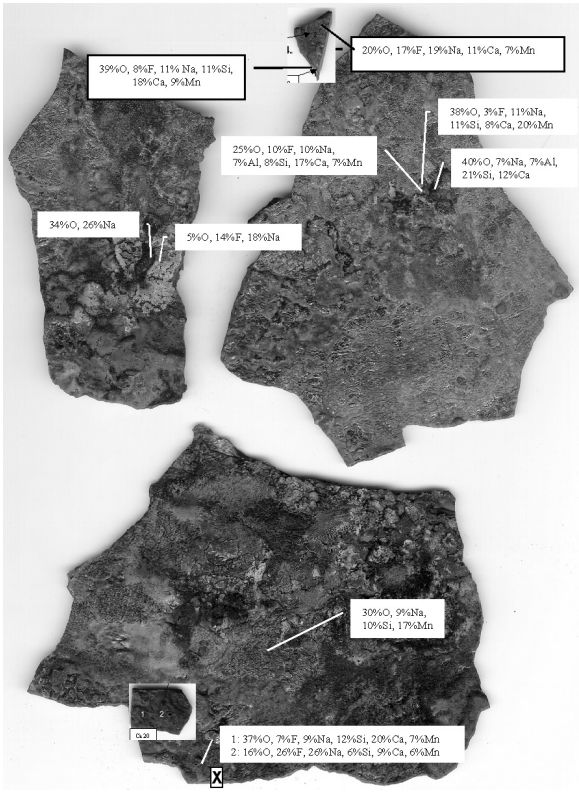


Figure 3: The appearance of the surface of a sample on the mould side is shown with concentrations of elements in some spots and with magnifications from some of the spots. Real height of this figure is about 20 cm

There are areas with no or low Ca content. This is due to the fact, that all Ca was in the form of cuspidine, and cupidine layer was next to the lubricating layer i.e., not in the layers next to the mould. Higher Ca content in some regions meant, that in the sampling more layers had remained stuck on the mould wall revealing cuspidine layer with higher Ca content.

After the end of casting and sampling of the *main* slag film, a *white* layer of film remained on the mould. This flamed when water was sprayed onto it indicating presence of elemental Na and/or K.

## HEAT TRANSFER

The heat transfer had a clear tendency to decrease during casting. Measured with the thermocouples it was observed, that the decrease in the heat transfer was small near the meniscus, but lower in the mould it could be significant.

Some heat transfer calculations were made to see, if the observed films could explain the temperatures measured with the thermocouples. An example is shown in Figure 5. The films used in the calculations are shown in Figure 4. They are representing films after different casting times at the distance of 39 cm below the meniscus. The case A is assumed film thickness after about 5 minutes of casting, the case B is a layer observed after 2 hours of casting and the case C is a layer observed after 5 hours of casting. Corresponding temperatures at the thermocouples were 110ºC, 78ºC and 62ºC and the calculated heat transfers 1220 kW/m$^2$, 700 kW/m$^2$ and 450 kW/m$^2$, respectively.

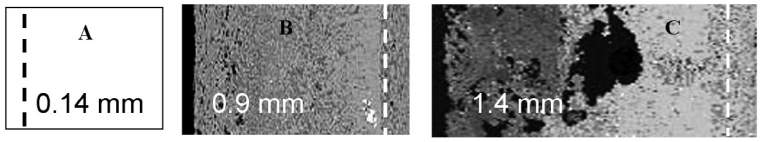


Figure 4: The films used in the heat transfer calculations (A, B and C). The total film thicknesses are shown

The calculations began from the cooling water and ended at the hot surface of the shell, i.e., to the solidus temperature of the stainless steel (calculated to be 1380ºC). The heat flux was set so that the temperature in the mould wall at the point of the thermocouple was the same temperature, which was measured with thermocouple in the same case. If the layer contained porosity, the conductivity of this layer was calculated based on the fractional areas of the solid material and pores

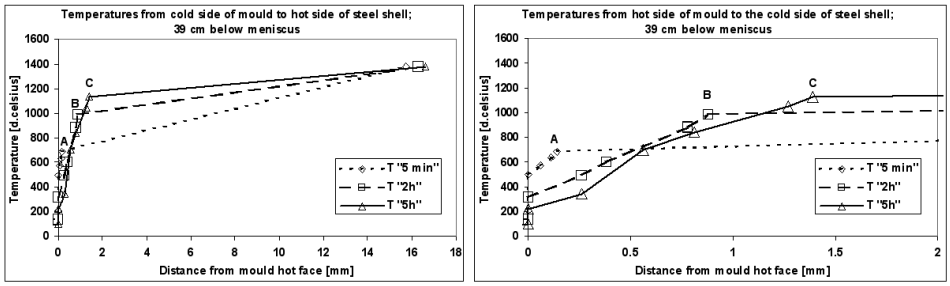


Figure 5: Calculated temperatures through the layers in films of three cases (A,B and C, see Figure 4) from hot surface of mould a) to the inner side of steel shell and b) to the hot surface of the steel shell. Obs. b) is part of a)

In the case C there are five different layers in the calculation, in the case B four and in the case A three. From these calculations, it is possible to state that the layers observed can serve as an explanation for the very low heat fluxes in some cases (i.e., low temperatures recorded).

## MINOR ELEMENTS IN THE MAIN PHASES

There was a tendency for those compounds of minor elements (impurities in powder, from steel or refractories, or added as tracer) to be distributed unevenly in the main phases. The main phases were for example cuspidine ($3CaO{\cdot}2SiO_2{\cdot}CaF_2$) or nepheline ($Na_3K(AlSiO_4)_4$), and minor elements were in this case Mg, Mn, Zr, S, K and Ti. Data used here were from the layers in the film shown in Figure 4C.

Figure 6 shows concentrations of minor elements against Ca concentration in the main phases (NaF phase was excluded). Ca was used to represent the type of main phase studied. If Ca-concentration in the main phase was over 20%, only Zr and Fe favoured those

phases. Other minor elements were higher in phases containing no Ca. The phase with approximately 21% Ca contained minor elements with moderate concentrations.

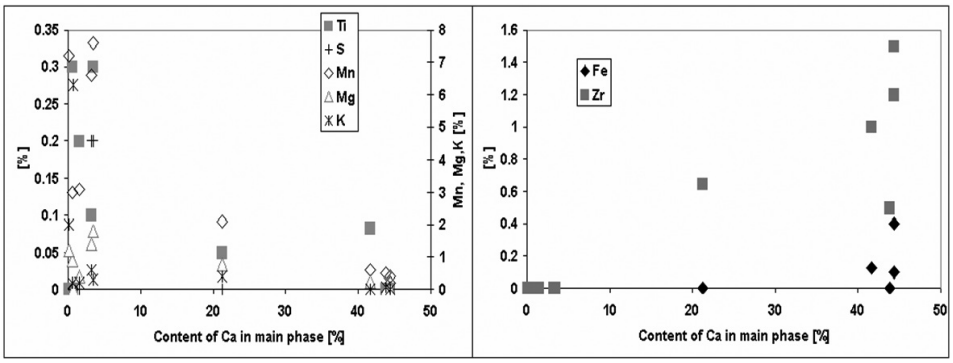


Figure 6: Concentrations of minor elements vs. Ca content in the main phases. Main phases (such as cuspidine) are *indicated* as based on Ca content of the phase

As Zr was used as a tracer, the phenomenon above makes it more difficult to read information from Zr concentrations. Phases containing no Ca contained no Zr either. Unfortunately, barium, which was also used as a tracer in this case, was not included in these field analyses. Concentrations of minor elements can give a hint as to the phase or compound concerned. For example, potassium (K) concentrations of over 2% probably indicate the presence of nepheline.

## PHASES IN THE FILM

In Figure 7 a detail from the film in Figure 4 case C is shown. In this figure all the main phases are present and this was one of the most complicated films. The phase showing high content of Ca was analysed to be cuspidine (1), the phase showing high content of Al was analysed to be nepheline (2) type (analysed contents of elements in mass%: O 39, F 0, Na 11, Si 18.6, Ca 0.7, Al 18.7, K 6.3, Mg 0) and the phase showing high content of Na and F was NaF (3).

The formation of cuspidine and nepheline could be expected as a result of slow cooling and solidification of the casting powder in question. Between 1 and 2 there is a transition area with a mix of two phases, but the interface between layers 2 and 3 is very sharp i.e., there is no transition area between those. That suggests, that NaF phase had formed with a special own mechanism. It is suggested, that the formation mechanism includes formation of NaF gas as one step and condensing of gas in the area near the *cold* mould wall. This mechanism could produce observed mono phase NaF and very sharp interface against nepheline dominating layer.

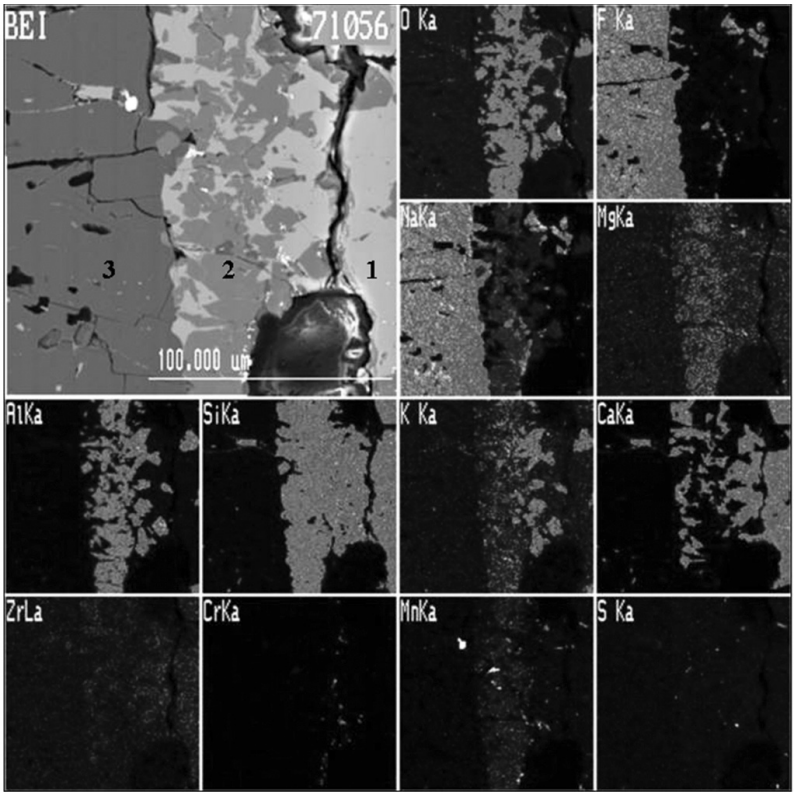


Figure 7: A backscatter electron image from *transition* area in a film showing changes in the contents of elements. Numbers are referring to different areas with different phases

## THE FILM WITH Ti STABILIZED STEEL GRADES

It is known that in the casting of Ti stabilized austenitic steel grades sticking of the steel shell to the mould wall occurs more often than with non Ti stabilized grades. In the flux films from casts of Ti stabilised steel grades, it is possible to observe the same basic principles as with non-Ti alloyed grades, both in appearance and in the concentration of elements. The main difference is the occurrence of a calcium titanate phase. An example of a film 15 cm below the meniscus is shown in Figure 8 with contents of some elements.

The whitish coloured layer with a high Ca concentration indicates the presence of a cuspidine phase. The slag layer with a dendritic structure on the right hand side was formed during the tail-out. The solidification rate has been the correct for dendritic growth. On the mould side of the cuspidine layer, there was a layer with a high concentration of Al, which was also fairly typical. In those composition points, where Al concentration has the highest value, K also has its highest values (not shown in this figure) and the Na/K ratio is 4.3 and 3.4, which indicates the presence of nepheline phase. The presence of nepheline is also a common feature in films from non-Ti alloyed grade casts.

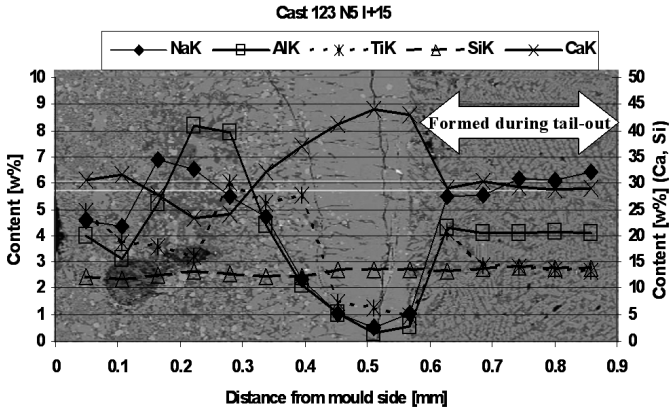


Figure 8: Layers in the film from cast of Ti alloyed steel grade. Concentrations of elements are drawn on the layers. The mould side is on the left. The layer with the dendritic structure formed during the tail-out (only part of that layer is in the Figure) [4].

The most significant difference when compared with steel grades without Ti alloying was the presence of small whitish spots of a calcium titanate phase ($CaTiO_3$); analyses revealed that all the Ti was in this form. Other phases did not, therefore, contained any Ti.

In Figure 9 it can be seen, that Ti causes faster growth of thickness of films and that lengths of films found were shorter than with non-Ti alloyed grades. Faster growth of film together with brittleness of film (found in sampling) leads sooner in to the unstable film and causes fracturing of the film, which for one leads to sticking of the shell on the mould.

Kashikawa *et al.* [3] proposed based on their investigation, that the results suggest that nucleants could be used to modify the crystallization behaviour of fluxes, because these slags can be undercooled significantly. Probably the formation of calcium titanate, acting as a nucleant, was accelerating the nucleation of other phases like dicalcium silicate and cuspidine, and undercooling of the liquid remained smaller, leading to faster growth of the film.

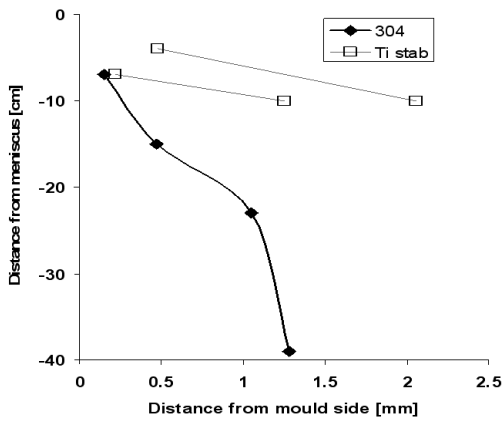


Figure 9: Thickness and length of some films from Ti stabilised casts and one from non-stabilised (to the shell side of the cuspidine rich layer, see also Figure 8)

## FRACTURING IN THE FILM

When the flux film is increasing in thickness, it can come into the state where it starts to fracture. In Figure 10 there are a solid, unbroken film, and two fractured films shown.

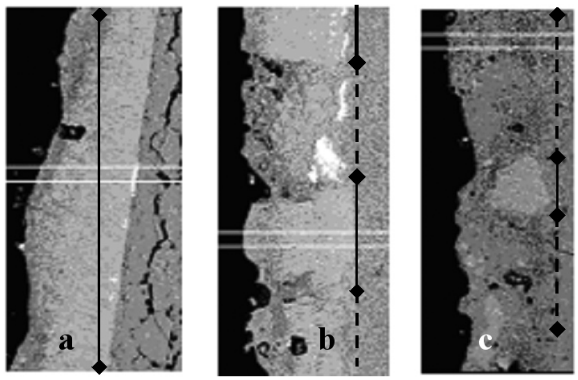


Figure 10: Examples of slag film structures showing unbroken and fractured films (a, b and c). Width of the sub figures is about 1 mm

Dash lines in Figure 10 indicate places in the film where there has been fractures and the film has been formed later. In Figure 10b the whitish cuspidine layer has broken into several short pieces. In the case c only some spots are left in the later formed film. Formation of the structures of the films shown in Figures 4B, 4C, 7 and 8 takes time, i.e., no fracturing has taken place and the film have hours of time to develop. White stripes are steel locating most often on the border between the film formed during the casting and the film formed during the tail-out.

## CONCLUSIONS

- The most typical feature in the sampled films was the layer in which the cuspidine phase was dominant.
- The films had a crystalline structure which either formed during solidification or via devitrification.
- When the cooling rate had been high enough and the residence time before sampling was short, glassy structures were also found.
- The most unexpected feature was the formation of a separate NaF layer, and the formation of elemental Na (and/or K) against the mould wall.
- It was shown that films can have long residence times (even hours) on the mould wall, and complex structures can develop, containing several sub layers, voids and pores.
- Evidence of fracturing was found in the sampled films.
- Surfaces on the mould side varied in appearance, not only between samples from different heats, but also locally in centimetre scale.

## REFERENCES

**Hooli, P.** (2007). *Study on the Layers in the Film Originating from the Casting Powder between Steel Shell and Mould and Associated Phenomena in Continuous Casting of Stainless Steel*. Doctoral Thesis, Helsinki University of Technology, Department of Materials Science and Engineering, Laboratory of Metallurgy, pp. 79. [1]

**Pesonen, K.** (1998). *Lubricating Layer in Continuous Casting of Stainless Steel*. Master's Thesis, University of Oulu, pp. 125. (in Finnish). [2]

**Kashiwaya, Y., Cicutti, C. E., Cramb, A. W. & Ishii, K.** (1998). *Development of Douple and Single Hot Thermocouple Technique for in Situ Observations and Measurement of Mould Slag Crystallization*. ISIJ International, Vol. 38, No. 4, pp. 348-356. [3]

**Jokisaari, J.** (2000). *Special Problems in Sequential Castings of Ti Stabilised Steels*. Master's Thesis, University of Oulu (2000), pp. 121. (in Finnish). [4]